NASA/TP–2010-216189

A Computational Framework to Control Verification and Robustness Analysis

Luis G. Crespo
National Institute of Aerospace, Hampton, Virginia

Sean P. Kenny and Daniel P. Giesy
Langley Research Center, Hampton, Virginia

January 2010

NASA STI Program . . . in Profile

Since its founding, NASA has been dedicated to the advancement of aeronautics and space science. The NASA scientific and technical information (STI) program plays a key part in helping NASA maintain this important role.

The NASA STI program operates under the auspices of the Agency Chief Information Officer. It collects, organizes, provides for archiving, and disseminates NASA's STI. The NASA STI program provides access to the NASA Aeronautics and Space Database and its public interface, the NASA Technical Report Server, thus providing one of the largest collections of aeronautical and space science STI in the world. Results are published in both non-NASA channels and by NASA in the NASA STI Report Series, which includes the following report types:

- TECHNICAL PUBLICATION. Reports of completed research or a major significant phase of research that present the results of NASA programs and include extensive data or theoretical analysis. Includes compilations of significant scientific and technical data and information deemed to be of continuing reference value. NASA counterpart of peer-reviewed formal professional papers, but having less stringent limitations on manuscript length and extent of graphic presentations.

- TECHNICAL MEMORANDUM. Scientific and technical findings that are preliminary or of specialized interest, e.g., quick release reports, working papers, and bibliographies that contain minimal annotation. Does not contain extensive analysis.

- CONTRACTOR REPORT. Scientific and technical findings by NASA-sponsored contractors and grantees.

- CONFERENCE PUBLICATION. Collected papers from scientific and technical conferences, symposia, seminars, or other meetings sponsored or co-sponsored by NASA.

- SPECIAL PUBLICATION. Scientific, technical, or historical information from NASA programs, projects, and missions, often concerned with subjects having substantial public interest.

- TECHNICAL TRANSLATION. English-language translations of foreign scientific and technical material pertinent to NASA's mission.

Specialized services also include creating custom thesauri, building customized databases, and organizing and publishing research results.

For more information about the NASA STI program, see the following:

- Access the NASA STI program home page at *http://www.sti.nasa.gov*

- E-mail your question via the Internet to help@sti.nasa.gov

- Fax your question to the NASA STI Help Desk at 443-757-5803

- Phone the NASA STI Help Desk at 443-757-5802

- Write to:
  NASA STI Help Desk
  NASA Center for AeroSpace Information
  7115 Standard Drive
  Hanover, MD 21076-1320

NASA/TP–2010-216189

A Computational Framework to Control Verification and Robustness Analysis

Luis G. Crespo
National Institute of Aerospace, Hampton, Virginia

Sean P. Kenny and Daniel P. Giesy
Langley Research Center, Hampton, Virginia

National Aeronautics and
Space Administration

Langley Research Center
Hampton, Virginia 23681-2199

January 2010

Available from:

NASA Center for AeroSpace Information
7115 Standard Drive
Hanover, MD 21076-1320
443-757-5802

Abstract

This paper presents a methodology for evaluating the robustness of a controller based on its ability to satisfy the design requirements. The framework proposed is generic since it allows for high-fidelity models, arbitrary control structures and arbitrary functional dependencies between the requirements and the uncertain parameters. The cornerstone of this contribution is the ability to bound the region of the uncertain parameter space where the degradation in closed-loop performance remains acceptable. The size of this bounding set, whose geometry can be prescribed according to deterministic or probabilistic uncertainty models, is a measure of robustness. The robustness metrics proposed herein are the parametric safety margin, the reliability index, the failure probability and upper bounds to this probability. The performance observed at the control verification setting, where the assumptions and approximizations used for control design may no longer hold, will fully determine the proposed control assessment.

Nomenclature

C	Complement set operator
$\boldsymbol{d}$	Design parameter
$\mathcal{E}$	Feasible design space
$\mathcal{F}$	Failure domain
$\bar{\boldsymbol{d}}$	Nominal design parameter
$f_{\boldsymbol{p}}(\boldsymbol{p})$	Probability density function
$F_{\boldsymbol{p}}(\boldsymbol{p})$	Cumulative distribution function
$\mathcal{Q}$	Robust design space
$\boldsymbol{g}$	Constraint function
$\mathcal{F}$	Failure domain
$\mathcal{I}$	Indicator function
$\boldsymbol{m}$	Aspect vector of a hyper-rectangle
$\mathcal{M}_{\boldsymbol{p}}$	Maximal set in physical space
$\mathcal{M}_{\boldsymbol{u}}$	Maximal set in standard normal space
n	Number of samples
$\boldsymbol{p}$	Uncertain parameter in physical space
$\bar{\boldsymbol{p}}$	Nominal parameter point in physical space
$\tilde{\boldsymbol{p}}$	Critical parameter point in physical space
P	Probability operator
$\mathcal{R}$	Hyper-rectangle
$\mathcal{S}$	Hyper-sphere
$\boldsymbol{u}$	Uncertain parameter in standard normal space
$\bar{\boldsymbol{u}}$	Nominal parameter point in standard normal space
$\tilde{\boldsymbol{u}}$	Critical parameter point in standard normal space
U	Parameter transformation to standard normal space
$\tilde{\alpha}$	Critical similitude ratio
α	Similitude ratio
β	Reliability index
Δ	Support set
Ω	Reference set
$\psi_{\boldsymbol{p}}$	Upper bound to the failure probability
Φ	Cumulative distribution function of a standard normal variable
ρ	Parametric safety margin

Acronyms

CPV	Critical Parameter Value
CSR	Critical Similitude Ratio
FORM	First Order Reliability Method
LQG	Linear Quadratic Gaussian
LTI	Linear Time Invariant
MS	Maximal Set
PID	Proportional-integral-derivative
PSM	Parametric Safety Margin
RI	Reliability index
SORM	Second Order Reliability Method

1 Introduction

Control verification is the last simulation-based step before control validation and experimental testing. As a result, a control verification setting entails complex, nonlinear, high-fidelity simulations where all subsystems, commonly developed independently having its own set of approximations, assumptions and methods, are integrated. Under these conditions, the vast majority of simplifications supporting robust and adaptive control methods — e.g., linear dynamics, multi-affine parameter dependencies, attainment of matching conditions — may not hold. The methodology proposed in this paper is applicable to variable-fidelity models of the plant while permitting arbitrary functional dependencies between the stability and performance requirements and the uncertainty. Note that the scope of this framework precludes the usage of convexity conditions from the outset.

Most of the strategies for robust control analysis are based on identifying the worst-case stability and performance of a Linear Time Invariant (LTI) system. While strategies for uncertainty in the mathematical form of the model, i.e., model-form uncertainty, are intrinsically conservative, those for real parameter uncertainties can only handle particular dependencies. Those strategies include affine, multi-affine [1,2] and polynomial forms [3,4]. The deployment of these methods over other functional forms is not possible without introducing unintended conservatism. Such conservatism is highly undesirable in control engineering where a balance between robustness and performance is essential.

For the aforementioned reasons, control verification is usually performed using sampling-based techniques such as Monte Carlo analysis [5–10]. However, when accurate robustness assessments are desired, the computational demands associated with these methods render them impractical. This is especially true when there are high-consequence low-probability events of interest, e.g., the probability of instability. The foundation of this paper is the bounding of regions in the uncertain parameter space where the closed-loop performance remains acceptable. In contrast to alternative approaches, the method enabling the identification of such regions is optimization-based. Furthermore, the problem formulation does not introduce conservatism into the resulting control assessment. The size of this bounding set, whose geometry can be prescribed according to deterministic or probabilistic uncertainty models, is a measure of robustness. Several of these measures are proposed herein. The implementation of the strategies proposed only requires a model of the closed-loop response that is continuously parametrized with the uncertainty, and a standard algorithm for constrained optimization.

This paper is organized as follows. Basic concepts and definitions are introduced in Section 2. This is followed by Section 3 where the mathematical background required to perform set deformations according to deterministic

uncertainty models is discussed. Extensions enabling the usage of probabilistic uncertainty models are presented in Sections 4 and 5. Finally, an example and a few concluding remarks close the paper.

2 Concepts and Definitions

The object of this paper is the evaluation of the robustness characteristics of a closed-loop system having a parametric mathematical model. The parameters which specify the system are grouped into two categories: uncertain parameters, denoted by the vector $\boldsymbol{p}$ and the control design parameters denoted by the vector $\boldsymbol{d}$. While the plant, actuator and sensor models depend on $\boldsymbol{p}$, the controller depends on $\boldsymbol{d}$.

The uncertainty model of $\boldsymbol{p}$ can be deterministic or probabilistic. A deterministic uncertainty model is prescribed by the *Uncertainty Set* Δ, while a probabilistic one is prescribed by a random vector. This vector is specified by the joint probability density function $f_{\boldsymbol{p}}(\boldsymbol{p})$ defined over Δ. The uncertainty set of the probabilistic model is commonly called the *Support Set.* Hereafter, the terms uncertainty set and support set will be used interchangeably. By specifying the uncertainty model, it is implied that Δ contains the actual value of $\boldsymbol{p}$, which is assumed to be time invariant. In principle, the uncertainty set can be unbounded and can even be the entire parameter space. In practical applications, the choice of this model is usually made by a discipline expert. Any member of the uncertainty set is called a *Realization.* The *Nominal Parameter* point, denoted as $\bar{\boldsymbol{p}} \in \Delta$, is an estimate of the value the uncertain parameter assumes under nominal operating conditions. The plant evaluated at the nominal parameter point will be called the *Nominal Plant.* Further, the set of control design parameters of a *Baseline Controller* will be denoted as $\bar{\boldsymbol{d}}$.

Stability and performance requirements for the closed-loop system will be prescribed by the set of constraint functions $\boldsymbol{g}(\boldsymbol{p}, \boldsymbol{d}) < \boldsymbol{0}$. The constraints in $\boldsymbol{g}$ may depend implicitly on time or frequency[1]. Throughout this paper, it is assumed that vector inequalities hold component wise. The larger the region in $\boldsymbol{p}$-space where $\boldsymbol{g}(\boldsymbol{p}, \bar{\boldsymbol{d}}) < \boldsymbol{0}$, the better the robustness of the baseline controller. In the ideal case, such a region contains the support set Δ.

Sets in the parameter and design spaces, instrumental to the developments that follow, are introduced next. The *Failure Domain* corresponding to the

[1]For instance, if a requirement is that the step response $y(\boldsymbol{p}, \boldsymbol{d}, t)$ must not exceed the upper envelope $\hat{y}(t)$, the corresponding constraint is given by

$$\boldsymbol{g} = \max_t \{y(\boldsymbol{p}, \boldsymbol{d}, t) - \hat{y}(t)\}.$$

Maximizations over t, such as this one, will be evaluated by selecting the largest value assumed by the argument at the discrete points of a time simulation. Hence, the evaluation of $\boldsymbol{g}$ will not entail solving an optimization problem per se.

baseline controller $\bar{\boldsymbol{d}}$ is given by[2]

$$\mathcal{F}(\bar{\boldsymbol{d}}) \triangleq \bigcup_{j=1}^{\dim(\boldsymbol{g})} \mathcal{F}^j(\bar{\boldsymbol{d}}) \tag{1}$$

where

$$\mathcal{F}^j(\bar{\boldsymbol{d}}) \triangleq \{\boldsymbol{p} : \boldsymbol{g}_j(\boldsymbol{p}, \bar{\boldsymbol{d}}) \geq 0\}. \tag{2}$$

The failure domain is the collection of parameter points for which the baseline controller violates at least one of the requirements. While Equation (1) defines the overall failure domain, Equation (2) defines the failure domain corresponding to the jth requirement. The *Non-Failure Domain* is the complement set of the failure domain and will be denoted[3] as $C(\mathcal{F})$. The names "failure domain" and "non-failure domain" are used because in the failure domain at least one constraint is violated while, in the non-failure domain, all constraints are satisfied. The level of robustness of a controller is related to the size and geometry of the non-failure domain. The *Feasible Design Space*, denoted as $\mathcal{E}$ and defined by

$$\mathcal{E}(\bar{\boldsymbol{p}}) \triangleq \{\boldsymbol{d} : \boldsymbol{g}(\bar{\boldsymbol{p}}, \boldsymbol{d}) < \boldsymbol{0}\}, \tag{3}$$

is the set of designs that satisfy the requirements for the nominal plant. The *Robust Design Space*, $\mathcal{Q}$, defined as

$$\mathcal{Q}(\Delta) \triangleq \{\boldsymbol{d} : \boldsymbol{g}(\boldsymbol{p}, \boldsymbol{d}) < \boldsymbol{0}, \forall \boldsymbol{p} \in \Delta\}, \tag{4}$$

is the set of designs that satisfy the requirements for all parameter realizations associated with a given uncertainty model. A controller will be called *Strictly Robust* if it belongs to $\mathcal{Q}(\Delta)$, i.e., if $\mathcal{F}$ and Δ do not intersect. Otherwise, the controller will be called *Non-Robust*. Note that $\mathcal{Q} \subset \mathcal{E}$ when $\bar{\boldsymbol{p}} \in \Delta$.

The formulations that follow depend on whether the baseline controller satisfies the requirements for the nominal plant or not. To make this distinction, the function

$$\gamma = \min_j \{\boldsymbol{h}_j\}, \tag{5}$$

where

$$\boldsymbol{h}_j = \begin{cases} 1 & \text{if } \boldsymbol{g}_j(\bar{\boldsymbol{p}}, \bar{\boldsymbol{d}}) < 0 \\ -1 & \text{otherwise.} \end{cases} \tag{6}$$

is introduced. The nominal closed-loop system satisfies the requirements for which $\boldsymbol{h}_j = 1$ and violates those for which $\boldsymbol{h}_j = -1$. When $\gamma = 1$, all the requirements are satisfied and $\bar{\boldsymbol{d}} \in \mathcal{E}$. In this case we want to determine the

[2]Throughout this paper, super-indices are used to denote a particular vector or set while sub-indices refer to vector components, e.g., $\boldsymbol{p}_i^j$ is the ith component of the vector $\boldsymbol{p}^j$.

[3]$C(\cdot)$ is the set complement operator.

separation between $\bar{\boldsymbol{p}} \in C(\mathcal{F})$ and the failure domain $\mathcal{F}$. The larger the separation, the better the robustness characteristics of the controller. When $\gamma = -1$, at least one of the requirements is violated. In this case we want to determine the separation between $\bar{\boldsymbol{p}} \in \mathcal{F}$ and the non-failure domain $C(\mathcal{F})$. The larger the separation, the worse the robustness characteristics of the controller.

3 Set Deformations in the Parameter Space

Let Ω be a set in $\boldsymbol{p}$-space, called the *Reference Set*, whose geometric center is the nominal parameter $\bar{\boldsymbol{p}}$. The geometry of Ω will be prescribed according to the uncertainty in $\boldsymbol{p}$.

For the sake of clarity, the presentation that follows concentrates on the case where the baseline controller is feasible, i.e., $\gamma = 1$. One of the tasks of interest is to assign a measure of robustness to $\bar{\boldsymbol{d}}$ based on measuring how much the reference set can be deformed before intersecting the failure domain. The *Homothetic Deformation* of Ω with respect to $\bar{\boldsymbol{p}}$ by a factor of $\alpha \geq 0$, is the set $\mathcal{H}(\Omega, \alpha) = \{\bar{\boldsymbol{p}} + \alpha(\boldsymbol{p} - \bar{\boldsymbol{p}}) : \boldsymbol{p} \in \Omega\}$. The factor α, is called the *Similitude Ratio*. While expansions are accomplished when $\alpha > 1$, contractions result when $0 \leq \alpha < 1$. Note that $\mathcal{H}(\Omega, 1) = \Omega$, and $\mathcal{H}(\Omega, \alpha_1) \subset \mathcal{H}(\Omega, \alpha_2)$ when $\alpha_1 < \alpha_2$. Hereafter, deformations must be interpreted as homothetic expansions or contractions about $\bar{\boldsymbol{p}}$.

Intuitively, one imagines that the reference set is being deformed until its boundary touches the failure domain, i.e., until at least one member of the deformed set violates one or several of the closed-loop requirements. Figure 1 shows a sketch for a hyper-rectangular reference set. Any point where the deforming set touches the failure domain is a *Critical Parameter Value* (CPV). The CPV, which will be denoted as $\tilde{\boldsymbol{p}}$, might not be unique. The deformed set is called the *Maximal Set* (MS) and will be denoted as $\mathcal{M}_{\boldsymbol{p}}$. By construction, all the points interior to the MS satisfy the closed-loop requirements. The *Critical Similitude Ratio* (CSR), denoted as $\tilde{\alpha}$, is the similitude ratio of the deformation leading to the MS. While the CSR is a non-dimensional number, the Parametric Safety Margin (PSM), denoted as ρ and defined in Section 3.3, is its dimensional equivalent. The values taken on by the CSR and the PSM are proportional to the size of the MS.

The calculation of the CPV requires solving an standard optimization problem[4]. Such a problem is non-convex when the dependency of $\boldsymbol{g}$ on $\boldsymbol{p}$ is nonlinear. In any non-convex optimization problem there is always the possibility of convergence to the non-global optimum[5]. When this occurs, the CPV re-

[4] All the optimization problems posed in this paper were implemented using the "fmincon" function of the Matlab optimization toolbox.

[5] Note that the First Order Reliability Method (FORM) and the Second Order Reliability Method (SORM) formulations [17] widely used in reliability analysis suffer from the very

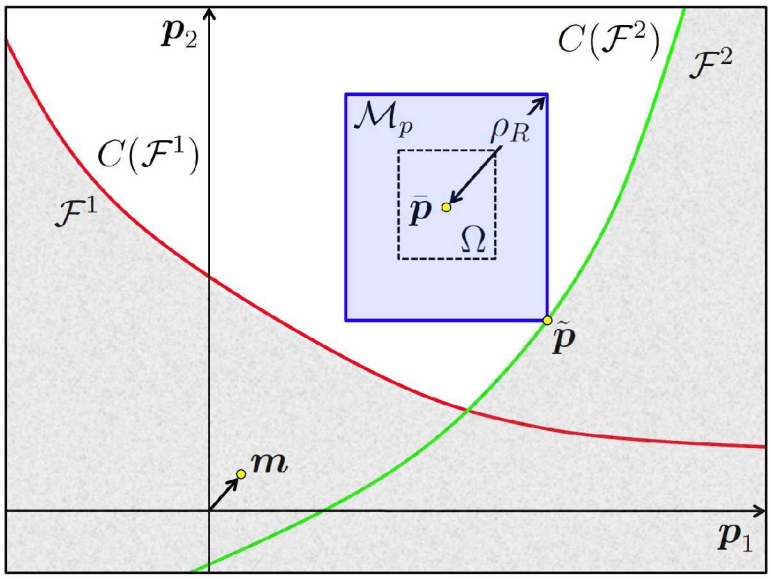

Figure 1. Variables in the deformation of a rectangular set for $\gamma = 1$. The failure domain is colored in gray.

sulting from the numerical optimization is mistaken and the corresponding MS intrudes into the failure region. This intrusion yields to a spuriously larger PSM. Absolute guarantees are not possible, but a variety of algorithmic safeguards can be used to deal with this deficiency. For instance, $\boldsymbol{g}$ can be evaluated at a few samples points in $\mathcal{M}_{\boldsymbol{p}}$ and if one happens to be in the failure domain, it can be used as an initial condition in a subsequent optimization. Requirements with an affine parameter dependency will not suffer from this potential drawback. Notice however, that such requirements may not only introduce unintended conservatism but also may misrepresent the desired control objective.

Formulations that enable finding the CPV for hyper-spherical and hyper-rectangular reference sets are presented next.

3.1 Deformation of Hyper-Spheres

One possible choice for the reference set Ω is the hyper-sphere

$$\mathcal{S}(\bar{\boldsymbol{p}}, R) = \{\boldsymbol{p} : \|\bar{\boldsymbol{p}} - \boldsymbol{p}\| \leq R\}\,, \tag{7}$$

where $\bar{\boldsymbol{p}}$ is its center and R is its radius. This geometry enables considering parameters with similar levels of uncertainty. These sets could also be used for parameters with dissimilar levels of uncertainty if scaling is used. However,

same deficiency.

whether scaling is used or not, a degree of dependence among parameters is introduced. The deformation of sets with this geometry can be performed as follows.

The CPV for the jth requirement is given by

$$\tilde{\boldsymbol{p}}^j = \underset{\boldsymbol{p}}{\operatorname{argmin}} \left\{ \|\boldsymbol{p} - \bar{\boldsymbol{p}}\| : \boldsymbol{h}_j \boldsymbol{g}_j(\boldsymbol{p}, \bar{\boldsymbol{d}}) \geq 0,\ A\boldsymbol{p} \geq \boldsymbol{b} \right\}. \tag{8}$$

The last constraint is used to exclude regions of the parameter space where plants are infeasible and/or uncertainty levels are unrealistic. For instance, if $\boldsymbol{p}$ is composed of masses and time-delays the constraint $\boldsymbol{p} \geq \boldsymbol{0}$ is implemented by using $A = I$, and $\boldsymbol{b} = \boldsymbol{0}$.

For $\gamma = 1$, the overall CPV is

$$\tilde{\boldsymbol{p}} = \tilde{\boldsymbol{p}}^k, \tag{9}$$

where

$$k = \underset{1 \leq j \leq \dim(\boldsymbol{g})}{\operatorname{argmin}} \left\{ \|\tilde{\boldsymbol{p}}^j - \bar{\boldsymbol{p}}\| \right\}. \tag{10}$$

Hence, the CPV for each individual requirement is identified and the closest of these CPVs to the nominal parameter point is the overall CPV. Notice that the critical requirement, i.e., any requirement that prevents a larger deformation, is $\boldsymbol{g}_k < 0$.

For $\gamma = -1$, the overall CPV is given by

$$\tilde{\boldsymbol{p}} = \underset{\boldsymbol{p}}{\operatorname{argmin}} \left\{ \|\boldsymbol{p} - \bar{\boldsymbol{p}}\| : \boldsymbol{g}(\boldsymbol{p}, \bar{\boldsymbol{d}}) \leq \boldsymbol{0},\ A\boldsymbol{p} \geq \boldsymbol{b} \right\}. \tag{11}$$

In this case, the value of $\tilde{\boldsymbol{p}}$ may not coincide with any of the $\tilde{\boldsymbol{p}}^j$s. This is because the overall CPV is at the intersection of the individual non-failure domains. Furthermore, if there exists a j such that $\tilde{\boldsymbol{p}}^j$ does not exist, meaning that the deformation grew unbounded, the overall CPV does not exist either. Note that for $\gamma = 1$, the CPV is the $\boldsymbol{p}$ point in the failure domain that is the closest to $\bar{\boldsymbol{p}}$, while for $\gamma = -1$ the CPV is the $\boldsymbol{p}$ point in the non-failure domain that is the closest to $\bar{\boldsymbol{p}}$. Figures 2 and 3 illustrate the $\gamma = 1$ and $\gamma = -1$ cases respectively. The failure domain, which is the union of both individual failure domains, is colored with gray.

The MS and the CSR are uniquely determined by the CPV according to

$$\mathcal{M}_{\boldsymbol{p}} = \mathcal{S}(\bar{\boldsymbol{p}}, \tilde{\alpha} R), \tag{12}$$

$$\tilde{\alpha} = \frac{\|\tilde{\boldsymbol{p}} - \bar{\boldsymbol{p}}\|}{R}. \tag{13}$$

Note that $\mathcal{M}_{\boldsymbol{p}}$ is the largest deformation of Ω which fits within $C(\mathcal{F})$ for $\gamma = 1$ and within $\mathcal{F}$ otherwise. The MS in figures 2 and 3 is shown as a blue circle.

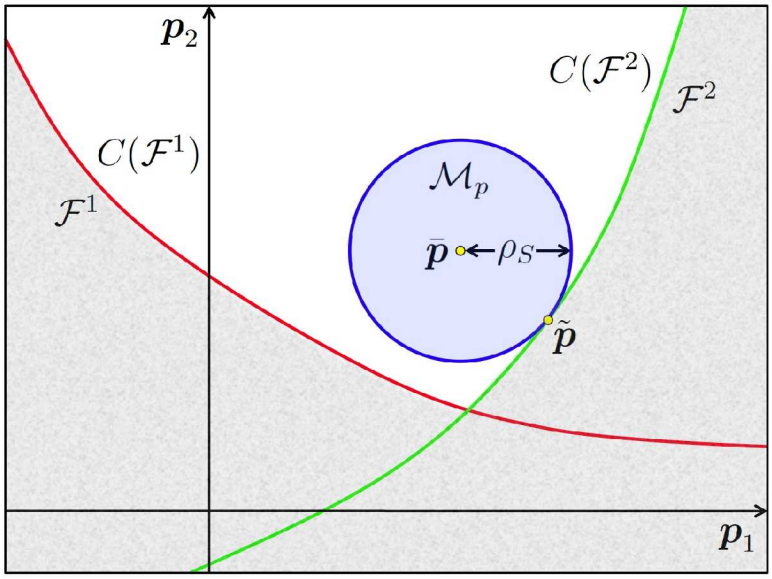

Figure 2. Relevant variables in the $\gamma = 1$ case. The failure domain and the maximal set are colored in gray and blue respectively.

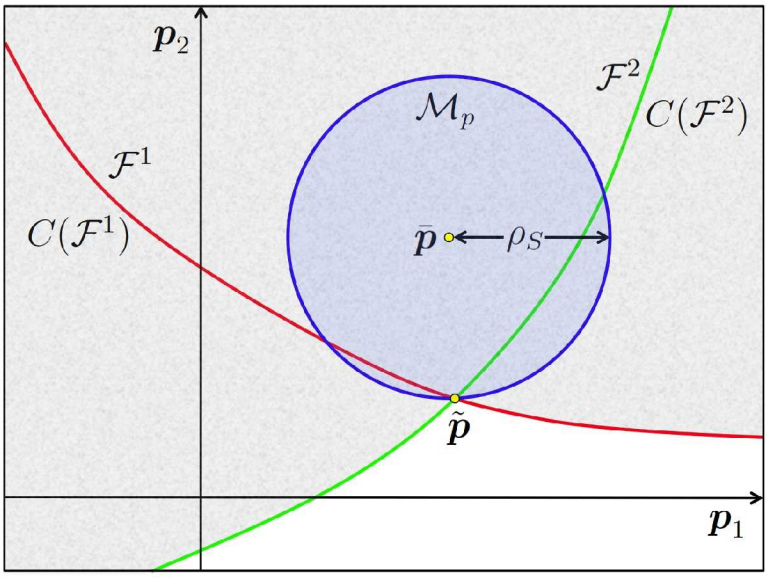

Figure 3. Relevant variables in the $\gamma = -1$ case. The failure domain and the maximal set are colored in gray and blue respectively.

In the particular case when $\dim\{\boldsymbol{p}\} = 1$, the MS is the interval $\mathcal{M}_{\boldsymbol{p}} = (\bar{p} - \rho, \bar{p} + \rho)$, where $\rho = |\bar{p} - \tilde{p}|$. Since this case only considers uncertainty in a single parameter, the resulting robustness metrics cannot capture the effects of the

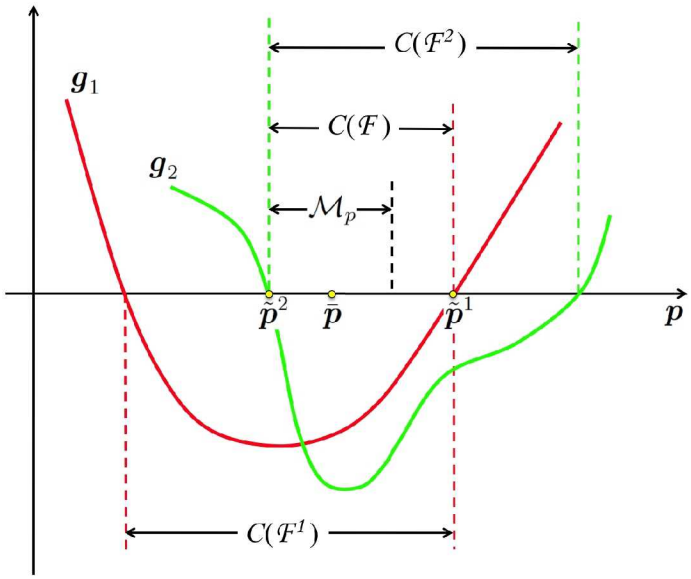

Figure 4. Relevant variables in a 1-dimensional setting.

interaction among such parameters on the requirements. Therefore, the CPV of a n dimensional deformation might be much closer to the nominal parameter point than the n one-dimensional CPVs resulting from deforming each of such parameters individually. The sketch in Figure 4 illustrates this setting for the design requirements $\boldsymbol{g}_1 < 0$ and $\boldsymbol{g}_2 < 0$. Note that the non-failure domain is the intersection of the individual non-failure domains. Besides, the overall CPV is the parameter point closest to the nominal point where at least one component of $\boldsymbol{g}$ is equal to zero. Since in the case shown this component is $\boldsymbol{g}_2$, $k = 2$ and $\tilde{p} = \tilde{p}^2$. Therefore, $\boldsymbol{g}_2 < 0$ is the critical requirement. Note that $\mathcal{M}_{\boldsymbol{p}}$, the MS corresponding to the overall CPV for which both constraints are active, is the intersection of the MSs associated with each individual constraint.

3.2 Deformation of Hyper-Rectangles

Another possible choice for the reference set Ω is the hyper-rectangle

$$\mathcal{R}(\bar{\boldsymbol{p}}, \boldsymbol{m}) = \{\boldsymbol{p} : \bar{\boldsymbol{p}} - \boldsymbol{m} \leq \boldsymbol{p} \leq \bar{\boldsymbol{p}} + \boldsymbol{m}\}\,, \tag{14}$$

where $\boldsymbol{m} > \boldsymbol{0}$ is the vector of half-lengths of the sides. Rectangular sets permit the consideration of parameters with dissimilar levels of uncertainty having no dependence. Such levels are attained by making $\boldsymbol{m}_i$ proportional to the level of uncertainty in $\boldsymbol{p}_i$.

Denote by $\|\boldsymbol{x}\|_{\boldsymbol{m}}^{\infty} \triangleq \max_i\{|\boldsymbol{x}_i|/\boldsymbol{m}_i\}$, the $\boldsymbol{m}$-scaled infinity norm. A distance between the vectors $\boldsymbol{x}$ and $\boldsymbol{y}$ can be defined as $\|\boldsymbol{x}-\boldsymbol{y}\|_{\boldsymbol{m}}^{\infty}$. Note that $\mathcal{R}(\bar{\boldsymbol{p}}, \boldsymbol{m}) =$

$\{\boldsymbol{p} : \|\boldsymbol{p} - \bar{\boldsymbol{p}}\|_{\boldsymbol{m}}^{\infty} \leq 1\}$. Formulations that enable deforming sets with this geometry are presented next.

The CPV in the hyper-rectangular case is given by Equations (8-11) after replacing the Euclidean norm with the $\boldsymbol{m}$-scaled infinity norm. The "max" resulting from this substitution can be eliminated by introducing the similitude ratio α defined earlier. This leads to the following expression for the jth individual CPV

$$\langle \tilde{\boldsymbol{p}}^j, \tilde{\alpha}^j \rangle = \underset{\boldsymbol{p},\alpha}{\operatorname{argmin}} \{\alpha : \ \boldsymbol{h}_j \boldsymbol{g}_j(\boldsymbol{p}, \bar{\boldsymbol{d}}) \geq 0, \ A\boldsymbol{p} \geq \boldsymbol{b}, \\ \bar{\boldsymbol{p}} - \alpha \boldsymbol{m} \leq \boldsymbol{p} \leq \bar{\boldsymbol{p}} + \alpha \boldsymbol{m}\}. \tag{15}$$

In this setting, the overall CPV is the individual CPV that is the closest to the nominal parameter point in the sense of the $\boldsymbol{m}$-scaled infinity norm.

The MS and the CSR are

$$\mathcal{M}_{\boldsymbol{p}} = \mathcal{R}(\bar{\boldsymbol{p}}, \tilde{\alpha}\boldsymbol{m}), \tag{16}$$

$$\tilde{\alpha} = \|\tilde{\boldsymbol{p}} - \bar{\boldsymbol{p}}\|_{\boldsymbol{m}}^{\infty}. \tag{17}$$

3.3 Robustness Metrics for Deterministic Uncertainty Models

Because the CSR measures the size of the MS, its value is proportional to the degree of robustness of the controller $\bar{\boldsymbol{d}}$ to uncertainty in $\boldsymbol{p}$. The CSR is a non-dimensional metric whose value depends on the size of the reference set. The PSM, which is the dimensional equivalent of the CSR, serves the same purpose without having this dependency. The *Spherical PSM* is

$$\rho_S(\tilde{\boldsymbol{p}}) \triangleq \gamma \tilde{\alpha} R, \tag{18}$$

where the CSR is given by Equation (13), while the *Rectangular PSM* is

$$\rho_R(\tilde{\boldsymbol{p}}) \triangleq \gamma \tilde{\alpha} \|\boldsymbol{m}\|, \tag{19}$$

where the CSR is given by Equation (17). The sign convention enforced by γ in these equations implies the following: if the PSM takes on a negative value, the controller does not even satisfy the requirements for the nominal plant. If the PSM is zero, the controller exhibits no robustness because there are arbitrarily small perturbations of $\boldsymbol{p}$ from $\bar{\boldsymbol{p}}$ leading to a constraint/requirement violation. If the PSM is positive, the requirements are satisfied by the nominal plant and those around it. The larger the PSM, the larger the Ω-shaped neighborhood of $\bar{\boldsymbol{p}}$ for which the requirements are satisfied.

The PSMs corresponding to individual requirements result from using $\tilde{\alpha}^j$ and $\boldsymbol{h}_j$, instead of $\tilde{\alpha}$ and γ, in Equations (18-19). This yields to

$$\rho_S(\tilde{\boldsymbol{p}}^j) \triangleq \boldsymbol{h}_j \|\tilde{\boldsymbol{p}}^j - \bar{\boldsymbol{p}}\|, \tag{20}$$

$$\rho_R(\tilde{\boldsymbol{p}}^j) \triangleq \boldsymbol{h}_j \|\tilde{\boldsymbol{p}}^j - \bar{\boldsymbol{p}}\|_{\boldsymbol{m}}^{\infty} \|\boldsymbol{m}\|. \tag{21}$$

The individual PSMs enable comparing the levels of robustness associated with each requirement. When $\gamma = 1$, the smallest individual PSM is equal to the overall PSM, i.e., $\rho(\tilde{\boldsymbol{p}}) = \min\{\rho(\tilde{\boldsymbol{p}}^j)\}$. When $\gamma = -1$ however, the smallest individual PSM is just an upper bound to the overall PSM, i.e., $\rho(\tilde{\boldsymbol{p}}) \leq \min\{\rho(\tilde{\boldsymbol{p}}^j)\}$. The trade-off between conflicting requirements will be reflected by the values taken on by the individual PSMs. Controllers that maximize the overall PSM will incidentally attain a trade-off that optimally balances the robustness for all requirements.

Traditionally, robust control analysis is made by setting forth an uncertainty set and checking if the stability and performance for all set members is satisfactory. This applies to methods for both, real parameter and model form uncertainty. Determination of whether a controller is robust or not for a given hyper-spherical or hyper-rectangular set Δ, is a matter of making $\Omega = \Delta$ and calculating the CSR. The controller is strictly robust if and only if the CSR is greater or equal to one. A controller might turn out to be non-robust because of an overly-large uncertainty set or because the requirements are too stringent. If the size of uncertainty model is not reduced, and the design requirements are not relaxed, the only choice is to adopt more complex control structures until a robust controller is found. This practice however, usually lead to high-order controllers. Alternatively, one may enable the usage of simpler control structures by allowing for requirements violations with a small probability. Strategies based on this idea are presented next.

4 Probabilistic Uncertainty Models

Hereafter, it is assumed that a probabilistic uncertainty model of $\boldsymbol{p}$ is available. Recall that such a model is prescribed by a random vector having the joint probability density function $f_{\boldsymbol{p}}(\boldsymbol{p})$, defined over the support set Δ. Note that the only information from such a model required for determining whether a controller is strictly robust or not is its support set. The developments that follow are suited for controllers that are non-robust. The analysis of such controllers entails quantifying the severity by which the requirements are violated. In the context of deterministic uncertainty models, one metric for this is the volume of $\Delta \cap C(\mathcal{M}_{\boldsymbol{p}})$.

Probabilistic uncertainty models enable the discrimination among all possible parameter realizations. The value of the joint density function at each particular realization can be interpreted as a measure of our belief that such a realization is the actual value of the uncertain parameter. In this setting, a natural metric of robustness is the probability of violating the design requirements. This probability, called the *Failure Probability*, will be denoted as $P[\mathcal{F}]$. The failure probability is zero for robust controllers, while it is greater

than zero for non-robust ones. Clearly, the smaller $P[\mathcal{F}]$, the more robust is the controller. Note that the set $\Delta \cap C(\mathcal{M}_{\boldsymbol{p}})$ above is an approximation of the failure domain and its volume is the failure probability for the case when uncertainties are uniformly distributed. It is worth noticing that a controller may attain a small value of $P[\mathcal{F}]$ but fail to satisfy the requirements for the nominal plant.

The developments that follow enable the comparison of controllers with varying levels of complexity from a practical perspective. For instance, if a simple Proportional-Integral-Derivative (PID) controller satisfies the closed-loop requirements for 99% of the plants, it is worth determining how much complexity are we willing to accept for that extra 1%. One may accept using a simpler, non-robust controller when the corresponding probability of failure is sufficiently small. The pursuit of zero failure probability usually leads to complex controllers whose robustness may be very close to that of much simpler ones for most of the plants.

In contrast to the contributions in [11–14] on probabilistic controls, the developments herein are not intended to alleviate the computational burden of pursuing robust stability, but to enable the discrimination among events in the set of all possible closed-loop system performances according to their chance of occurrence. This has the potential to address and alleviate the demands on the controller complexity imposed by worst-case control policies. In this regard, this paper is better aligned with the developments in References [8–10] and with the idea of handling some of the requirements as soft constraints [15, 16].

5 Set Deformations in Standard Normal Space

The calculation of probabilities can be better performed in spaces other than $\boldsymbol{p}$-space. The most relevant of these spaces is the standard normal space, commonly referred to as the $\boldsymbol{u}$-space. In $\boldsymbol{u}$-space, the multi-variate probability density function is an uncorrelated normal density function with zero mean and unit standard deviation, whose value decreases as $\exp(-\|\boldsymbol{u}\|^2/2)$. For most probability distributions, there is a probability preserving parameter transformation [17], denoted hereafter as $\boldsymbol{u} = U(\boldsymbol{p})$, that maps the requirements from $\boldsymbol{p}$-space to $\boldsymbol{u}$-space such that $P[U(\mathcal{F})] = P[\mathcal{F}]$.

The formulations introduced in Section 3 that enable the deformation of sets in $\boldsymbol{p}$-space can be easily extended to the $\boldsymbol{u}$-space. In this setting, the sets $\mathcal{S}(\bar{\boldsymbol{u}}, R)$ and $\mathcal{R}(\bar{\boldsymbol{u}}, \boldsymbol{m})$ will be used as reference sets. A natural choice is $\bar{\boldsymbol{u}} = \boldsymbol{0}$ because in the standard normal space most of the probability is concentrated about the origin. An obvious parallelism between the concepts, notions and equations introduced earlier and the ones in $\boldsymbol{u}$-space is apparent. For instance,

if $\Omega = \mathcal{S}(\bar{\boldsymbol{u}}, R)$ the CPV corresponding to the jth requirement is given by

$$\tilde{\boldsymbol{u}}^j = \underset{\boldsymbol{u}}{\operatorname{argmin}} \left\{ \|\boldsymbol{u} - \bar{\boldsymbol{u}}\| : \boldsymbol{h}_j \boldsymbol{g}_j(U^{-1}(\boldsymbol{u}), \bar{\boldsymbol{d}}) \geq 0 \right\}, \tag{22}$$

where $\boldsymbol{h}_j$ results from using Equation (6) with $\bar{\boldsymbol{p}} = U^{-1}(\bar{\boldsymbol{u}})$. Note that this equation is analogous to Equation (8). The constraint $A\boldsymbol{p} \geq \boldsymbol{b}$ is no longer used since its intent can now be achieved by using a suitable Δ in $f_{\boldsymbol{p}}(\boldsymbol{p})$. Note that if the baseline controller is robust, $U(\mathcal{F})$ is empty and all the optimization problems posed in this section have no feasible solution.

The formulation for the overall CPVs can be easily inferred from the above developments, e.g., for $\gamma = 1$ the overall CPV is $\tilde{\boldsymbol{u}} = \tilde{\boldsymbol{u}}^k$, where k results from using $\|\tilde{\boldsymbol{u}}^j - \bar{\boldsymbol{u}}\|$ in Equation (10). The MS and the CSR corresponding to hyper-spherical sets are

$$\mathcal{M}_{\boldsymbol{u}} = \mathcal{S}(\bar{\boldsymbol{u}}, \tilde{\alpha} R), \tag{23}$$

$$\tilde{\alpha} = \frac{\|\tilde{\boldsymbol{u}} - \bar{\boldsymbol{u}}\|}{R}, \tag{24}$$

while those for hyper-rectangular sets are

$$\mathcal{M}_{\boldsymbol{u}} = \mathcal{R}(\bar{\boldsymbol{u}}, \tilde{\alpha} \boldsymbol{m}), \tag{25}$$

$$\tilde{\alpha} = \|\tilde{\boldsymbol{u}} - \bar{\boldsymbol{u}}\|_{\boldsymbol{m}}^{\infty}. \tag{26}$$

Note that $\mathcal{M}_{\boldsymbol{u}}$ is the largest deformation of Ω which fits within $U(C(\mathcal{F}))$ for $\gamma = 1$ and within $U(\mathcal{F})$ otherwise.

5.1 Robustness Metrics for Probabilistic Uncertainty Models

Metrics based on probabilistic uncertainty models and methods for their calculation are introduced next.

5.1.1 Reliability Indices

The Reliability Index (RI) is the analogous to the PSM in $\boldsymbol{u}$-space. In particular, the *Spherical RI* is defined as

$$\beta_S(\tilde{\boldsymbol{u}}) \triangleq \gamma \tilde{\alpha} R, \tag{27}$$

where the CSR is given by Equation (24), while the *Rectangular RI* is

$$\beta_R(\tilde{\boldsymbol{u}}) \triangleq \gamma \tilde{\alpha} \|\boldsymbol{m}\|, \tag{28}$$

where the CSR is given by Equation (26). The RIs corresponding to individual requirements are

$$\beta_S(\tilde{\boldsymbol{u}}^j) \triangleq \boldsymbol{h}_j \|\tilde{\boldsymbol{u}}^j - \bar{\boldsymbol{u}}\|, \tag{29}$$

$$\beta_R(\tilde{\boldsymbol{u}}^j) \triangleq \boldsymbol{h}_j \|\tilde{\boldsymbol{u}}^j - \bar{\boldsymbol{u}}\|_{\boldsymbol{m}}^{\infty} \|\boldsymbol{m}\|. \tag{30}$$

As with the PSMs, $\beta(\tilde{\boldsymbol{u}}) = \min\{\beta(\tilde{\boldsymbol{u}}^j)\}$ for $\gamma = 1$ and $\beta(\tilde{\boldsymbol{u}}) \leq \min\{\beta(\tilde{\boldsymbol{u}}^j)\}$ for $\gamma = -1$.

In $\boldsymbol{p}$-deformations, all the information on the relative levels of uncertainty in the components of $\boldsymbol{p}$ is determined by the geometry of the reference set. In $\boldsymbol{u}$-deformations, this information is prescribed by both the reference set and the probability density function. To preserve the relative levels of uncertainty of the probabilistic model, the reference set should be a hyper-sphere or a hyper-cube centered at the origin. Note however, that the geometry of the reference set can be adjusted as desired. The developments in the next section indicate that reference sets leading to large maximal sets are desirable. Such sets may not preserve the uncertainty levels implied by $f_{\boldsymbol{p}}(\boldsymbol{p})$. Strategies for the calculation of upper bounds to the failure probability based on the deformations of sets in $\boldsymbol{p}$- and $\boldsymbol{u}$-space are presented next.

5.1.2 Bounds to Failure Probability

Let us define $\psi \triangleq P[C(\mathcal{M})] = 1 - P[\mathcal{M}]$, where $\mathcal{M}$ is a MS in either $\boldsymbol{p}$- or $\boldsymbol{u}$-space. Note that $P[\mathcal{F}] \leq \psi$ for $\gamma = 1$ since $\mathcal{F} \subseteq C(\mathcal{M})$. Furthermore, $P[\mathcal{F}] \geq 1 - \psi$ for $\gamma = -1$ since $\mathcal{M} \subseteq \mathcal{F}$. For the reminder of this section our discussion concentrates on the case where $\gamma = 1$ so ψ is an upper bound to $P[\mathcal{F}]$.

For deformations in $\boldsymbol{p}$-space we will use the notation

$$\psi_{\boldsymbol{p}} = 1 - P[\mathcal{M}_{\boldsymbol{p}}]. \tag{31}$$

If the components of $\boldsymbol{p}$ are independent random variables and $\Omega = \mathcal{R}(\bar{\boldsymbol{p}}, \boldsymbol{m})$, we obtain

$$\psi_{\boldsymbol{p}}(\bar{\boldsymbol{p}}, \boldsymbol{m}, \rho_R) = 1 - \prod_{i=1}^{\dim(\boldsymbol{p})} \left[F_{\boldsymbol{p}_i}\left(\bar{\boldsymbol{p}}_i + \frac{|\rho_R|\boldsymbol{m}_i}{\|\boldsymbol{m}\|}\right) - F_{\boldsymbol{p}_i}\left(\bar{\boldsymbol{p}}_i - \frac{|\rho_R|\boldsymbol{m}_i}{\|\boldsymbol{m}\|}\right) \right], \tag{32}$$

where $F_{\boldsymbol{p}}$ is the cumulative distribution function and ρ_R is given by Equation (19). Upper bounds to $P[\mathcal{F}^j]$ can be calculated by using the individual PSMs from Equation (21) into Equation (32). Since $\mathcal{M}_{\boldsymbol{p}}$ and therefore ρ_R, are independent of the uncertainty model $f_{\boldsymbol{p}}$, upper bounds corresponding to different uncertainty models can be calculated with minimal computational effort.

Tighter bounds are obtained if the reference set chosen leads to a more probable MS. This can be easily attained by working in the standard normal space. For deformations in $\boldsymbol{u}$-space we will use the notation

$$\psi_{\boldsymbol{u}} = 1 - P[\mathcal{M}_{\boldsymbol{u}}]. \tag{33}$$

While $\psi_{\boldsymbol{p}}$ can be estimated analytically for hyper-rectangular sets, $\psi_{\boldsymbol{u}}$ can be estimated analytically for hyper-spherical sets centered at $\bar{\boldsymbol{u}} = \boldsymbol{0}$ and for

hyper-rectangles. The following Lemma [6] enables the calculation of $\psi_{\boldsymbol{u}}$ for the former case.

Lemma 1. *If $\boldsymbol{u}_i$ for $i = 1, 2, \ldots, l$ is a set of independent standard normal variables, $\Lambda(l, r) \triangleq P[\|\boldsymbol{u}\| \leq r]$ is given by*

$$\Lambda(l,r) = \begin{cases} \operatorname{erf}\left(\frac{r}{\sqrt{2}}\right) - e^{-\frac{r^2}{2}} \sqrt{\frac{2}{\pi}} \sum_{i=1}^{\frac{l-1}{2}} \frac{r^{l-2i}}{(l-2i)!!} & \text{if } l \text{ is odd} \\ 1 - e^{-\frac{r^2}{2}} \sum_{i=1}^{\frac{l}{2}} \frac{r^{l-2i}}{(l-2i)!!} & \text{if } l \text{ is even} \end{cases} \tag{34}$$

where !! is the double factorial operator[7]*.*

In the case where $\Omega = \mathcal{S}(\bar{\boldsymbol{u}}, R)$ and $\bar{\boldsymbol{u}} = \boldsymbol{0}$, Equations (33-34) lead to

$$\psi_{\boldsymbol{u}}(\beta_S) = 1 - \Lambda(\dim(\boldsymbol{p}), |\beta_S|). \tag{36}$$

Upper bounds to $P\left[\mathcal{F}^j\right]$ can be calculated by using the individual RIs from Equation (29) into Equation (36).

In the case where $\Omega = \mathcal{R}(\bar{\boldsymbol{u}}, \boldsymbol{m})$, we have

$$\psi_{\boldsymbol{u}}(\bar{\boldsymbol{u}}, \boldsymbol{m}, \beta_R) = 1 - \prod_{i=1}^{\dim(\boldsymbol{p})} \left[\Phi\left(\bar{\boldsymbol{u}}_i + \frac{|\beta_R| \boldsymbol{m}_i}{\|\boldsymbol{m}\|} \right) - \Phi\left(\bar{\boldsymbol{u}}_i - \frac{|\beta_R| \boldsymbol{m}_i}{\|\boldsymbol{m}\|} \right) \right], \tag{37}$$

where Φ is the cumulative distribution function of a standard normal random variable and β_R is given by Equation (28). Upper bounds to $P[\mathcal{F}^j]$ can be calculated by using the individual RIs from Equation (30) into Equation (37). Because of the parameter transformation $\boldsymbol{u} = U(\boldsymbol{p})$, the calculation of $\psi_{\boldsymbol{u}}$ for a new uncertainty model $f_{\boldsymbol{p}}$ requires solving for a new $\mathcal{M}_{\boldsymbol{u}}$ and therefore for a new RI. This is in contrast to the bound in Equation (32) where a change in $f_{\boldsymbol{p}}$ can be readily accommodated for.

Because the bounds result from calculating the probability of an event their value lies between zero and one, i.e., $\psi_{\boldsymbol{p}} \in (0, 1]$ and $\psi_{\boldsymbol{u}} \in (0, 1]$. For a given $f_{\boldsymbol{p}}$, $\boldsymbol{g}$ and $\bar{\boldsymbol{d}}$, there is no general rule that determines which reference set leads to the smallest upper bound. Equations (32), (36) and (37) are guaranteed upper bounds to the failure probability and as such they do not suffer from approximation error. Note that the efficiency of the methods used to calculate the PSMs, the RIs and the bounds is independent of the value of $P[\mathcal{F}]$.

[6] The corresponding proof is available in reference [18].

[7] The double factorial [19] is defined as

$$n!! = \begin{cases} n \cdot (n-2) \cdots 5 \cdot 3 \cdot 1 & n > 0 \text{ and odd} \\ n \cdot (n-2) \cdots 6 \cdot 4 \cdot 2 & n > 0 \text{ and even} \\ 1 & n = -1, 0 \end{cases} \tag{35}$$

5.1.3 Failure Probability

The problem of finding $P[\mathcal{F}]$, or equivalently $P[U(\mathcal{F})]$, is usually difficult since it requires evaluating a multi-dimensional integral over a complex integration domain. Methods for approximating the failure probability include sampling based techniques, FORM [17], SORM and the hybrid method [18, 20]. An outline of the latter approach follows.

The hybrid method approximates the failure probability by combining sampling with the bounds derived above. Once the MS has been determined, an arbitrary sample point of $f_{\boldsymbol{p}}$ can be easily tested for membership in this set. If the sample point lies within the MS, it is unnecessary to go through the computational expense of evaluating $\boldsymbol{g}$, since the outcome is now known. The numerical advantage of using this method is a consequence of not having to evaluate $\boldsymbol{g}$ at these realizations. In particular,

$$P[\mathcal{F}] \approx \frac{(1-\gamma)(1-\psi)}{2} + \frac{\gamma\psi}{n}\sum_{i=1}^{n}\mathcal{I}(\boldsymbol{p}^i, \mathcal{F}), \tag{38}$$

where ψ is given by Equation (32), (36) or (37), $\boldsymbol{p}^i$ for $i = 1, 2, \ldots n$ are samples of $f_{\boldsymbol{p}}$ in $C(\mathcal{M})$, and $\mathcal{I}$ is the indicator function

$$\mathcal{I}(\boldsymbol{p}, \mathcal{F}) = \begin{cases} 1 & \text{if } \boldsymbol{p} \in \mathcal{F} \\ 0 & \text{otherwise.} \end{cases} \tag{39}$$

An approximation to $P\left[\mathcal{F}^j\right]$ results from using the variables corresponding to the jth requirement. For instance, if $\Omega = \mathcal{R}(\bar{\boldsymbol{p}}, \boldsymbol{m})$, we have

$$P\left[\mathcal{F}^j\right] \approx \frac{(1-\boldsymbol{h}_j)(1-\psi_{\boldsymbol{p}})}{2} + \frac{\boldsymbol{h}_j\psi_{\boldsymbol{p}}}{n}\sum_{i=1}^{n}\mathcal{I}(\boldsymbol{p}^i, \mathcal{F}^j), \tag{40}$$

where $\psi_{\boldsymbol{p}}$ results from substituting the ρ_R in Equation (21) into Equation (32) and every $\boldsymbol{p}^i$ falls into $C(\mathcal{R}(\bar{\boldsymbol{p}}, \|\tilde{\boldsymbol{p}}^j - \bar{\boldsymbol{p}}\|_{\boldsymbol{m}}^{\infty}\boldsymbol{m}))$. Note that Equation (1) implies that $P[\mathcal{F}] \geq \max\{P[\mathcal{F}^j]\}$. More efficient implementations of the hybrid method are available [18, 20].

This method is especially advantageous when the number of evaluations of $\boldsymbol{g}$ required to determine the MS is considerably less than the number of samples falling within the MS. This is usually the case when $P[\mathcal{F}] \ll 1$. While the efficiency of the method increases with the CSR, its accuracy is comparable to the one of Monte Carlo using floor(n/ψ) samples [20]. A particularly attractive feature of the hybrid method is that its efficiency and accuracy does not depend on the robustness of the controller [20]. This sharply contrasts with the case in sampling-based methods, where accurate robustness assessments (i.e., those requiring statistics having small confidence intervals) demand a number of samples that grow exponentially fast as $P[\mathcal{F}]$ approaches zero. Figure 5 illustrates the dependency of the Monte Carlo approximation P_f to $P[\mathcal{F}]$ on

the minimum number of samples required to attain an upper limit of the 95% confidence interval equal to $2P_f$. Note that accurate approximations to small failure probabilities require an exceedingly high number of $\boldsymbol{g}$ evaluations.

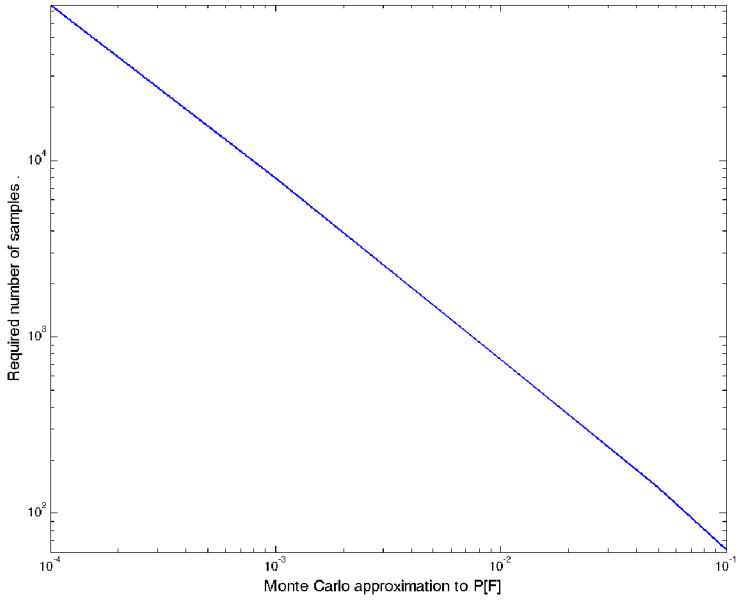

Figure 5. Number of samples required to accurately approximate failure probabilities via Monte Carlo sampling.

While the RIs and the upper bounds to the failure probability have a notion of robustness based on the closeness of the nominal parameter point to the failure domain, the failure probability does not. As such, the estimation of $P[\mathcal{F}]$ does not require the definition of a nominal parameter point and designs attaining small failure probabilities may have their corresponding failure domain close to regions where $f_{\boldsymbol{p}}(\boldsymbol{p})$ is large. While a small $P[\mathcal{F}]$ is desirable, only a sizable value of the RI guarantees that the nominal parameter point is separated from $\mathcal{F}$. While the reduction of $P[\mathcal{F}]$ does not necessarily increase this separation, an increase of the RI not only augments the separation but also reduces $P[\mathcal{F}]$.

6 Example

The comparative analysis of controllers designed for the robust control challenge problem posed in the 1990 American Control Conference [21] is presented next. This problem was chosen because the public availability of the controllers

enable the reproducibility of the results. Note however, that the methodology developed is applicable to far more complex problems than the one herein.

The benchmark system, shown in Figure 6, is a two-mass/spring system with a non-collocated sensor actuator pair. Several design problems were posed

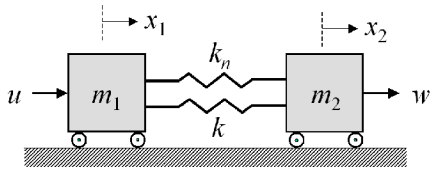

Figure 6. Two-mass spring system.

based on this setting. As in Reference [22], additional uncertainties are considered to fully exercise the scope of the methodology. We added a non-linear spring with constant k_n, a time delay τ denoting a first-order lag between controller command and actuator response and a control effectiveness uncertainty f resulting from variation in sensors, control gain and actuator failure. Hence, $\boldsymbol{p} = [m_1, m_2, k, k_n, \tau, f]^\top$. The plant model is

$$\begin{aligned}
\dot{x}_1 &= x_3 \\
\dot{x}_2 &= x_4 \\
\dot{x}_3 &= \frac{k}{m_1}(x_2 - x_1) + \frac{k_n}{m_1}(x_2 - x_1)^3 + \frac{fu}{m_1}, \\
\dot{x}_4 &= \frac{k}{m_2}(x_1 - x_2) + \frac{k_n}{m_2}(x_1 - x_2)^3 + \frac{w}{m_2}, \\
\tau\dot{u} &= u_c - u.
\end{aligned}$$

Stability and performance requirements, prescribed as

1. Local closed-loop stability.
2. Settling time: the output to a unit-impulse disturbance w must fall between ± 0.1 after 15s.
3. Control saturation: the control for a unit-impulse disturbance must fall between ± 1.

lead to

$$\boldsymbol{g} = \left[\max_{1 \le i \le n_p} \{\Re(s^i)\},\ \max_{t>15}\{|x_2|\} - 0.1,\ \max_{t>0}\{|u|\} - 1 \right]^\top,$$

where s^i is a closed-loop pole of the linearized system and $\Re(\cdot)$ is the real part operator. Eleven controllers designed by several authors using different

Controller	Gain margin	Phase margin	$\rho_R(\tilde{\boldsymbol{p}}^1)$	$\rho_R(\tilde{\boldsymbol{p}}^2)$	$\rho_R(\tilde{\boldsymbol{p}}^3)$	$\rho_R(\tilde{\boldsymbol{p}})$
	db	deg	Stability	Settling time	Saturation	Overall
A	2.5	-20.6	0.320	-0.019	0.368	less than zero
B	3.2	26.7	0.490	-0.175	0.523	less than zero
C	3.3	26.6	0.501	-0.189	0.533	less than zero
D	15.1	57.2	0.562	0.212	$-\infty$	less than zero
E	2.4	22.2	0.394	-0.259	0.233	less than zero
F	5.2	23.9	0.419	0.012	-3.277	less than zero
H	3.4	24.8	0.510	-0.005	0.524	less than zero
W_1	3.3	24.5	0.501	0.001	0.517	0.001
W_2	6.0	34.2	0.754	-0.024	0.639	less than zero
B_1	1.8	18.9	0.300	0.020	0.003	0.003
B_2	2.8	27.2	0.437	0.038	0.141	0.038

Table 1. Stability margins and PSMs.

methods are studied here. These controllers will be labeled as A, B, C, D, E, F and H (from [22] and references therein); W_1 and W_2 (from [23]); and B_1 and B_2 (from [24]). The structure of the controllers is as follows: controllers A, B, and C used loop transfer recovery; controllers D, H, W_1 and W_2 are based on H-infinity control; controller E is designed by optimization; controller F is Linear Quadratic Gaussian (LQG) based; and controllers B_1 and B_2 were designed using μ-synthesis.

The deformation of the reference set $\Omega = \mathcal{R}(\bar{\boldsymbol{p}}, \boldsymbol{m})$ is considered first. We assume that $\bar{\boldsymbol{p}} = [1, 1, 1, 0, 0, 1]^\top$ and $\boldsymbol{m} = [4, 4, 5, 2, 1, 2]^\top$, e.g., we expect four times more uncertainty in the value of the masses than in the value of the time delay. The pair $\langle \bar{\boldsymbol{p}}, \boldsymbol{m} \rangle$, which constitutes a deterministic uncertainty model, is, as any mathematical model of uncertainty, subjective. Notice however, that the MS for $\gamma = 1$ is fully contained in the non-failure domain regardless of the value this pair takes on. In order to prevent deformations leading to infeasible plants, the constraints $m_1 > 0$, $m_2 > 0$, $k > 0$, $\tau > 0$ and $f > 0$ in the form of $A\boldsymbol{p} \geq \boldsymbol{b}$ were added. Table 1 presents the stability margins for the nominal plant and the PSMs for the three requirements. Results on Table 1 show that only W_1, B_1 and B_2 satisfy the requirements for the nominal plant (i.e., the PSMs are positive). While W_2 has the best figure of merit in regard to stability and control saturation, the settling time requirement is best satisfied by D. Note that the stability margins are not reliable indicators of robust stability. For instance, while D has the best stability margins, it does not attain the largest $\rho_R(\tilde{\boldsymbol{p}}^1)$. According to the PSM, B_2 is the best controller since it attains the largest $\rho_R(\tilde{\boldsymbol{p}})$, which is 0.038.

Control assessments for a probabilistic uncertainty model are presented

Controller	$\beta_S(\tilde{\boldsymbol{u}}^1)$ Stability	$\beta_S(\tilde{\boldsymbol{u}}^2)$ Settling time	$\beta_S(\tilde{\boldsymbol{u}}^3)$ Saturation	$\beta_S(\tilde{\boldsymbol{u}})$ Overall
A	0.665	-0.037	0.913	less than zero
B	0.992	-0.319	1.169	less than zero
C	1.01	-0.336	1.191	less than zero
D	2.366	0.598	$-\infty$	less than zero
E	0.690	-3.517	0.374	less than zero
F	1.627	0.025	$-\infty$	less than zero
H	1.050	-0.009	1.174	less than zero
W_1	1.027	0.0009	1.152	0.0009
W_2	2.147	-0.072	2.287	less than zero
B_1	0.497	0.030	0.005	0.005
B_2	0.852	0.066	0.236	0.066

Table 2. Spherical RIs.

next. We assume that m_1, m_2, k, k_n, τ and f are independent, Beta-distributed random variables with shape parameters, $[5,5]$, $[5,5]$, $[2,3.7]$, $[6,6]$, $[0.3,5]$ and $[1,1]$ and support sets $[0,2]$, $[0,2]$, $[0.5,2]$, $[-0.5,0.5]$, $[0,0.1]$ and $[0.5,1.5]$, respectively. The value of $\boldsymbol{h}$ corresponding to $\bar{\boldsymbol{u}} = \boldsymbol{0}$ makes the signs of the individual PSMs and RIs to coincide.

The deformation of $\Omega = \mathcal{S}(\bar{\boldsymbol{u}}, R)$ for $\bar{\boldsymbol{u}} = \boldsymbol{0}$ leads to the metrics shown in Table 6. According to the RIs, the controller D is the one with best stability and settling time characteristics while W_2 has the best figure of merit for control saturation. According to the RI, B_2 is the best controller since it attains the largest $\beta_S(\tilde{\boldsymbol{u}})$, which is 0.066. The bounds to the failure probability can be readily calculated from the entries of Table 6 and Equation (36). The control assessment resulting from these bounds coincide with the one based on the RIs.

The values of $P[\mathcal{F}^j]$, calculated using the hybrid method for $n = 1000$ samples and the RIs in Table 6, are shown in Table 6. Note that D has the best robustness in regard to the stability and settling time requirements, while W_2 is the best for control saturation. The values of $P[\mathcal{F}]$ for W_1, B_1 and B_2 are 0.908, 0.980 and 0.873 respectively. Recall that $\mathcal{F}$ is the union of all individual failure domains, and as such it cannot be calculated from the data in Table 6. According to the failure probability, B_2 is the best controller since it attains the smallest $P[\mathcal{F}]$, which is 0.873. Since the failure probabilities are large, the advantage of using the hybrid method is moderate.

Note that all the figures of merit provide consistent robustness assessments. The individual PSMs and RIs indicate not only which is the limiting design requirement, but more importantly, how the levels of robustness corresponding to all requirements compare among themselves.

Controller	$P[\mathcal{F}^1]$ Stability	$P[\mathcal{F}^2]$ Sett. time	$P[\mathcal{F}^3]$ Saturation
A	0.272	0.971	0.158
B	0.143	0.957	0.119
C	0.130	0.967	0.104
D	0.007	0.333	1
E	0.219	0.999	0.426
F	0.080	0.871	1
H	0.138	0.914	0.188
W_1	0.119	0.907	0.174
W_2	0.014	0.875	0.010
B_1	0.313	0.976	0.601
B_2	0.196	0.798	0.462

Table 3. Failure probabilities.

7 Concluding Remarks

This paper proposes a computational framework for evaluating the robustness of a controller based on its ability to satisfy the design requirements. The framework developed is applicable to linear and non-linear systems subject to stability and performance requirements having an arbitrary functional dependency on the uncertainty. These metrics are the parametric safety margin, the reliability index, the failure probability and upper bounds to this probability. The methods used to calculate these metrics are based on the solution of standard optimization problems. The parametric safety margin evaluates the robustness characteristics of the controller according to a deterministic uncertainty model. The other metrics, which require a probabilistic uncertainty model, account for the chance of occurrence of any given plant within the uncertainty set and therefore for the likelihood of unsatisfactory closed-loop performance. As compared to sampling-based methods, the efficiency of the tools used to calculate the proposed metrics is independent of the value they take on. This is particularly advantageous when the controllers are highly robust, a case when the computational expense of an accurate sampling-based analysis is impractical. The proposed methodology enables a fair comparison of controllers designed using different methods and assumptions. The justification for adopting complex control architectures and the determination of the consequences of violating such assumptions are aspects that can be naturally evaluated using this framework.

Acknowledgement

This work was supported by the National Aeronautics and Space Administration under the NRAs NNH07ZEA001N and NNX07AC48A of NASA of the Hypersonics and Integrated Resilient Aircraft Control (IRAC) Projects. The authors would like to thank Carey Butrill, Suresh Joshi, Brian Mason and Lucas Horta for their diligence in the review of this manuscript.

References

1. Barmish, B. R.: New tools for robustness analysis. *Proceedings of the 27th Conference on Decision and Control, Austin, Texas*, 1988, pp. 1–6.

2. deGaston, R.; and Sofonov, M.: Exact calculation of the multiloop stability margin. *IEEE Transactions on Automatic Control*, vol. 33, no. 2, 1988, pp. 156–171.

3. Babayigit, A. H.; Ross, B. R.; and Shcherbakov, P. S.: On robust stability with nonlinear parameter dependence: some benchmark problems illustrating the dilation integral method. *Proceedings of the 2004 American Control Conference*, Boston, Massachusetts, 2004, pp. 2671–2673.

4. Barmish, B. R.; and Shcherbakov, P. S.: A dilation method for robustness problems with nonlinear parameter dependence. *Proceedings of the American Control Conference, Denver, Colorado*, 2003, pp. 3834–3839.

5. Bryson, A. E.; and Mills, R. A.: Linear-Quadratic-Gaussian controllers with specified parameter robustness. *AIAA Journal of Guidance, Control and Dynamics*, vol. 21, no. 1, 1998, pp. 11–18.

6. Darligton, J.; Pantelides, C.; Rustem, B.; and Tanyi, B.: An algorithm for constrained nonlinear optimization under uncertainty. *Automatica*, vol. 35, 1999, pp. 217–228.

7. Ray, L.; and Stengel, R.: A Monte Carlo approach to the analysis of control system robustness. *Automatica*, vol. 29, 1993, pp. 229–236.

8. Tenne, D.; and Singh, T.: Efficient minimax control design for prescribed parameter uncertainty. *AIAA Journal of Guidance, Control and Dynamics*, vol. 27, no. 6, 2004, pp. 1009–1016.

9. Wang, Q.; and Stengel, R. F.: Robust control of nonlinear systems with parametric uncertainty. *Automatica*, vol. 38, 2002, pp. 1591–1599.

10. Wang, Q.; and Stengel, R. F.: Robust nonlinear flight control of a high performance aircraft. *IEEE Transactions on Automatic Control*, vol. 13, no. 1, 2005, pp. 15–26.

11. Blondel, V.D.; and J.N.Tsitsiklis: A survey of computational complexity results in systems and control. *Automatica*, vol. 36, 2000, pp. 1249–1274.

12. Calafiore, G.; Dabbene, F.; and Tempo, R.: Randomized algorithms for probabilistic robustness with real and complex structured uncertainty. *IEEE Transactions on Automatic Control*, vol. 45, no. 12, December 2000, pp. 2218–2235.

13. Polyak, B.; and Tempo, R.: Probabilistic robust design with linear quadratic regulators. *Systems and Control Letters*, vol. 43, 2001, pp. 343–353.

14. Raghavan, V.; and Barmish, B. R.: Stability of systems with random parameters. *Proceedings of the 45th Conference on Decision and Control, San Diego, California*, 2006, pp. 3180–3185.

15. Barmish, B. R.; and Shcherbakov, P. S.: On avoiding vertexization of robustness problems: the approximate feasibility concept. *IEEE Transactions on Automatic Control*, vol. 47, no. 5, 2002, pp. 819–824.

16. Lagoa, C. M.: A convex-parameterization of risk-adjusted stabilizing controllers. *Automatica*, vol. 39, 2003, pp. 1829–1835.

17. Rackwitz, R.: Reliability analysis, a review and some perspectives. *Structural Safety*, vol. 23, 2001, pp. 365–395.

18. Crespo, L. G.; Giesy, D. P.; and Kenny, S. P.: Reliability-based Analysis and Design via Failure Domain Bounding. *Structural Safety*, vol. 31, 2009, pp. 306–315.

19. Weisstein, Eric W. Double Factorial. From MathWorld – A Wolfram Web Resource. `http://mathworld.wolfram.com/DoubleFactorial.html`.

20. Giesy, D. P.; Crespo, L. G.; and Kenny, S. P.: Approximation of failure probability using conditional sampling. *Proceedings of the 12th AIAA/ISSMO Multidisciplinary Analysis and Optimization Conference*, Victoria, Canada, AIAA-2008-5946.

21. Wie, B.; and Bernstein, D.: A benchmark problem for robust control design. *Proceedings of the 1990 American Control Conference*, San Diego, CA, USA, 1990, vol. 1, pp. 961–962.

22. Stengel, R. F.; and Morrison, C.: Robustness of solutions to a benchmark control problem. *AIAA Journal of Guidance, Control and Dynamics*, vol. 15, no. 5, 1992, pp. 1060–1067.

23. Wie, B.; Liu, Q.; and Byun, K.: Robust H-infinity control synthesis method and its application to benchmark problems. *AIAA Journal of Guidance, Control, and Dynamics*, vol. 15, no. 5, 1992, pp. 1140–1148.

24. Braatz, R.; and Morari, M.: Robust control for a noncollocated spring-mass system. *Journal of Guidance, Control and Dynamics*, vol. 15, no. 5, 1992, pp. 1103–110.

REPORT DOCUMENTATION PAGE

Form Approved
OMB No. 0704-0188

1. REPORT DATE *(DD-MM-YYYY)*	2. REPORT TYPE	3. DATES COVERED *(From - To)*
01-01-2010	Technical Publication	

4. TITLE AND SUBTITLE
A Computational Framework to Control Verification and Robustness Analysis

5a. CONTRACT NUMBER

5b. GRANT NUMBER

5c. PROGRAM ELEMENT NUMBER

6. AUTHOR(S)
Crespo, Luis G.; Kenny, Sean P.; Giesy, Daniel P.

5d. PROJECT NUMBER

5e. TASK NUMBER

5f. WORK UNIT NUMBER
457280.02.07.07.06.01

7. PERFORMING ORGANIZATION NAME(S) AND ADDRESS(ES)
NASA Langley Research Center
Hampton, VA 23681-2199

8. PERFORMING ORGANIZATION REPORT NUMBER
L-19786

9. SPONSORING/MONITORING AGENCY NAME(S) AND ADDRESS(ES)
National Aeronautics and Space Administration
Washington, DC 20546-0001

10. SPONSOR/MONITOR'S ACRONYM(S)
NASA

11. SPONSOR/MONITOR'S REPORT NUMBER(S)
NASA/TP-2010-216189

12. DISTRIBUTION/AVAILABILITY STATEMENT
Unclassified - Unlimited
Subject Category 08
Availability: NASA CASI (443) 757-5802

13. SUPPLEMENTARY NOTES

14. ABSTRACT

This paper presents a methodology for evaluating the robustness of a controller based on its ability to satisfy the design requirements. The framework proposed is generic since it allows for high-fidelity models, arbitrary control structures and arbitrary functional dependencies between the requirements and the uncertain parameters. The cornerstone of this contribution is the ability to bound the region of the uncertain parameter space where the degradation in closed-loop performance remains acceptable. The size of this bounding set, whose geometry can be prescribed according to deterministic or probabilistic uncertainty models, is a measure of robustness. The robustness metrics proposed herein are the parametric safety margin, the reliability index, the failure probability and upper bounds to this probability. The performance observed at the control verification setting, where the assumptions and approximizations used for control design may no longer hold, will fully determine the proposed control assessment.

15. SUBJECT TERMS
Verification; Uncertainty; Robustness Analysis; Monte Carlo

16. SECURITY CLASSIFICATION OF:			17. LIMITATION OF ABSTRACT	18. NUMBER OF PAGES	19a. NAME OF RESPONSIBLE PERSON
a. REPORT	b. ABSTRACT	c. THIS PAGE			STI Help Desk (email: help@sti.nasa.gov)
					19b. TELEPHONE NUMBER *(Include area code)*
U	U	U	UU	31	(443) 757-5802